UC Santa Barbara
UC Santa Barbara Previously Published Works

Title

Quantitative measurements of protein−surface interaction thermodynamics

Permalink

https://escholarship.org/uc/item/06d9q7j0

Journal

Proceedings of the National Academy of Sciences of the United States of America, 115(33)

ISSN

0027-8424

Authors

Kurnik, Martin
Ortega, Gabriel
Dauphin-Ducharme, Philippe
et al.

Publication Date

2018-08-14

DOI

10.1073/pnas.1800287115

Peer reviewed

Quantitative measurements of protein–surface interaction thermodynamics

Martin Kurnik[a,b], Gabriel Ortega[a,b,c], Philippe Dauphin-Ducharme[a,b], Hui Li[a,b,d], Amanda Caceres[a,b], and Kevin W. Plaxco[a,b,1]

[a]Department of Chemistry and Biochemistry, University of California, Santa Barbara, CA 93106; [b]Center for Bioengineering, University of California, Santa Barbara, CA 93106; [c]Protein Stability and Inherited Disease Laboratory, Center for Cooperative Research in Biosciences CIC bioGUNE, 48170 Derio, Spain; and [d]Engineering Research Center of Nano-Geomaterials of Ministry of Education, Faculty of Materials Science and Chemistry, China University of Geosciences, Wuhan 430074, China

Whereas proteins generally remain stable upon interaction with biological surfaces, they frequently unfold on and adhere to artificial surfaces. Understanding the physicochemical origins of this discrepancy would facilitate development of protein-based sensors and other technologies that require surfaces that do not compromise protein structure and function. To date, however, only a small number of such artificial surfaces have been reported, and the physics of why these surfaces support functional biomolecules while others do not has not been established. Thus motivated, we have developed an electrochemical approach to determining the folding free energy of proteins site-specifically attached to chemically well-defined, macroscopic surfaces. Comparison with the folding free energies seen in bulk solution then provides a quantitative measure of the extent to which surface interactions alter protein stability. As proof-of-principle, we have characterized the FynSH3 domain site-specifically attached to a hydroxyl-coated surface. Upon guanidinium chloride denaturation, the protein unfolds in a reversible, two-state manner with a free energy within 2 kJ/mol of the value seen in bulk solution. Assuming that excluded volume effects stabilize surface-attached proteins, this observation suggests there are countervening destabilizing interactions with the surface that, under these conditions, are similar in magnitude. Our technique constitutes an unprecedented experimental tool with which to answer long-standing questions regarding the molecular-scale origins of protein–surface interactions and to facilitate rational optimization of surface biocompatibility.

protein folding | protein–surface interactions | square wave voltammetry | biophysics | biosensors

Interactions between proteins and surfaces play important roles in nature, medicine, and biotechnologies. In the cell, for example, as much as 25% of even a relatively small proteome is estimated to interact with a membrane surface at some point in its life cycle (1). Some of these interactions are critical to metabolism and signal transduction, as exemplified by cytochrome *c* (2) and G proteins (3), both of which associate with membranes as part of their function. Protein–surface interactions can also prove detrimental, as exemplified by the membrane-mediated structural changes in proteins implied in neurodegenerative diseases, such as Alzheimer's (4) and Parkinson's disease (5, 6). Proteins also tend to unfold on and irreversibly adhere to artificial surfaces (7, 8), limiting the extent to which we can leverage protein functionality in human technologies, such as biosensors, tissue engineering scaffolds, protein microarrays, and drug delivery vehicles.

To date, the number of quantitative experimental studies of the thermodynamics with which proteins interact with specific surfaces has been limited, limiting, in turn, our understanding of why proteins retain function on some surfaces but irreversibly unfold and lose function on others. That is, in contrast to the extensive literature describing the extent to which adsorption alters protein structure (e.g., refs. 9 and 10) or seeking to empirically identify surfaces upon which proteins do not adhere and lose function (7, 8), quantitative, thermodynamic characterization of protein–surface interactions remains almost entirely limited to theoretical or computational studies (e.g., refs. 11–13). Here, however, we present an experimental approach for measuring the extent to which interactions with a chemically well-defined, macroscopic surface alter the stability of a protein (Fig. 1), using it to measure the extent to which interactions with a hydroxyl-coated surface alter the thermodynamic stability of a single-domain protein.

Results

As the test bed to establish our method, we have employed the SH3 domain of human Fyn tyrosine kinase (FynSH3), a widely studied 61-residue protein whose folding in bulk solution is well approximated as two-state (14, 15). To determine the protein's folding free energy when interacting with a surface, we attached a redox-active methylene blue to a carboxyl terminal cysteine residue (Fig. 1 and *SI Appendix*, Fig. S1), providing a means of monitoring its folding electrochemically. To site-specifically attach the protein to a well-defined macroscopic surface, we employed a variant in which the wild-type protein's two lysines are replaced with arginine (referred to simply as "FynSH3" hereinafter), thus rendering the amino terminus the only free amino group. We modified this with a seven-carbon alkane thiol through amide bond formation, allowing for deposition onto a gold surface via the formation of a gold–thiol bond.

Significance

Protein–surface interactions play important roles across biology, medicine, and biotechnologies. Specifically, while proteins are often found associated with biological surfaces in the cell (e.g., biomembranes), where they retain their structure and augment surface function, proteins tend to unfold on and irreversibly adhere to artificial surfaces, limiting our ability to leverage their functionality in technologies such as biosensors, tissue engineering scaffolds, and drug delivery vehicles. In response, we describe here an experimental approach by which we can measure the thermodynamic consequences of protein–surface interactions, suitable for answering long-standing questions regarding the physicochemical origins of these interactions. The resulting understanding should facilitate rational optimization of the biocompatibility of artificial surfaces used in a wide range of biomolecule-based technologies.
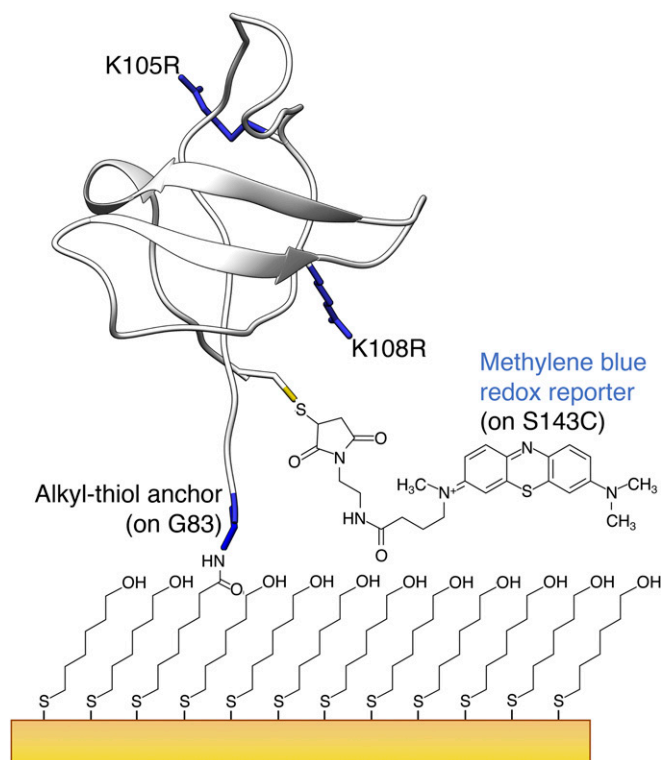
Fig. 1. We have measured the folding thermodynamics of a simple, well-characterized protein, FynSH3, site-specifically attached to a hydroxyl-coated macroscopic surface. To do so, we attached the protein to a hydroxyl-terminated alkane thiol SAM on a gold electrode using a unique primary amine on the amino terminus. Of note is that such SAMs can be terminated with any of a large number of functional groups (16), and thus our approach can access a wide range of surface chemistries. A methylene blue conjugated to a cysteine residue serves as a reporter that can be used to electrochemically monitor denaturant-induced unfolding, from which we can estimate the folding free energy of the surface-attached protein. Shown is the FynSH3 variant we have employed, in which the wild-type protein's lysine residues are replaced with arginines to leave the amino terminus a unique site for surface attachment via amide bond formation. Residue numbering is as per the full-length human Fyn protein.

To perform our studies on a chemically well-defined surface, we deposited the thiol-modified protein onto a gold electrode that we then treated with a six-carbon thiol. This creates a well-packed self-assembled monolayer (SAM) that can be terminated by any of a wide range of functional groups, providing access to a broad spectrum of surface chemistries (16). As our test bed surface, we employed a hydroxyl-terminated alkane thiol to produce a homogeneously hydroxyl-coated surface (Fig. 1). We selected this surface because it has been extensively characterized and is used in many technologies (16), including a range of biosensors (e.g., ref. 17).

The topology of FynSH3 places its termini in close proximity, ensuring that the native state positions the carboxyl-terminal methylene blue reporter near the surface (Fig. 1). Unfolding thus reduces the probability of the methylene blue being close to the surface, reducing the rate of electron transfer to the underlying gold electrode. Here we have used square-wave voltammetry to monitor this, as the technique is particularly sensitive to changes in electron transfer kinetics (Fig. 2 and *SI Appendix*, Fig. S2 and *Signal Optimization*). Specifically, when we perform square-wave voltammetry at a frequency of 500 Hz (Fig. 2*A*), rendering the approach sensitive to the more rapid electron transfer associated with the native protein, we observe a large faradaic peak under native conditions that is significantly reduced in the presence of 7.8 M guanidinium chloride (GdmCl). Conversely, when we perform square-wave

voltammetry at frequencies below ~15 Hz, rendering the approach more sensitive to the slower electron transfer associated with the unfolded state, the faradaic peak instead increases upon the addition of GdmCl (Fig. 2 *B* and *C* and *SI Appendix*, Fig. S2). As required for the determination of folding free energy, this denaturant-induced unfolding is fully reversible (Fig. 2*A* and *SI Appendix*, Fig. S3), and produces a denaturation curve (Fig. 3*A*) that, as is true for the protein in bulk solution (15), is well approximated as a simple, two-state process in which only the native and fully unfolded states are appreciably populated (18, 19).

Fitting the GdmCl denaturation curve to a two-state model, we obtain the folding free energy of the surface-attached protein. Specifically, under the conditions we have employed, the surface-attached protein is stable by 23.1 ± 0.5 kJ/mol (the values and uncertainties reported here and elsewhere in this work represent averages and 95% confidence intervals derived from multiple independent replicates). The GdmCl *m*-value of the surface-attached protein, a measure of the extent to which each 1-M increase in the concentration of this denaturant alters its folding free energy (18, 19), is -6.1 ± 0.1 kJ·mol^{-1}·M^{-1}. That is, each additional molar increase in GdmCl concentration shifts the equilibrium ~10-fold toward the unfolded state.

To ascertain the extent to which surface interactions alter the stability of FynSH3, we compared the folding free energy of the surface-attached protein to that of the protein when it is free in bulk solution (Fig. 3*B*). To measure the latter, we have used tryptophan fluorescence to monitor GdmCl-induced unfolding under the same conditions we employed on the surface. Doing so, we find that the protein's stability and GdmCl *m*-value in bulk solution are 24.6 ± 2.5 kJ/mol and -6.1 ± 0.6 kJ·mol^{-1}·M^{-1}, respectively. These values suggest that the thermodynamic consequences of surface attachment are, at 1.5 ± 1.8 kJ/mol, statistically insignificant. This said, the wide confidence intervals associated with this claim stem primarily from the precision with which our bulk solution experiments define the protein's *m*-value. If we instead assume that the protein adopts the same *m*-value in bulk solution as it does when surface-attached (the unconstrained, best-fit parameters are within error of one another), then interaction with this surface destabilizes the native protein by 1.8 ± 0.3 kJ/mol, a value that, while small, nevertheless achieves statistical significance. Irrespective of the validity or invalidity of this assumption, however, it appears that, in the presence of GdmCl, the folding of FynSH3 is, at most, only minimally destabilized by interaction with this surface.

To further support our claim that the GdmCl-induced response we observe for the surface-attached protein is accurately reporting on its folding free energy, we have also characterized the folding thermodynamics of a sequence variant, I50L. This hydrophobic core mutation is both chemically "neutral" (in terms of net charge and total hydrophobic surface area) and completely buried in the native state (20, 21), suggesting that it is unlikely to affect interactions with the surface. Thus, if our approach is accurately reporting on folding free energies, the energetic consequences of the substitution should be the same irrespective of whether the protein is on the surface or free in bulk solution. Consistent with this, the thermodynamic consequences associated with the substitution are 7.7 ± 2.6 kJ/mol and 7.8 ± 3.2 kJ/mol, respectively (Fig. 4 and *SI Appendix*, Table S1).

The observation that surface attachment so little alters the folding free energy of FynSH3 is counter to the expectation that excluded volume effects would stabilize the surface-attached protein by reducing the entropy of the unfolded state. Assuming a Kuhn length of 10 residues for the unfolded protein (22), excluded volume effects would be predicted to stabilize FynSH3 by ~9 kJ/mol (23–25). The absence of such stabilization suggests that there are other, similarly large destabilizing contributions arising due to interactions with the surface. In particular, we expect some destabilizing interactions to arise due to electrostatics (26). That
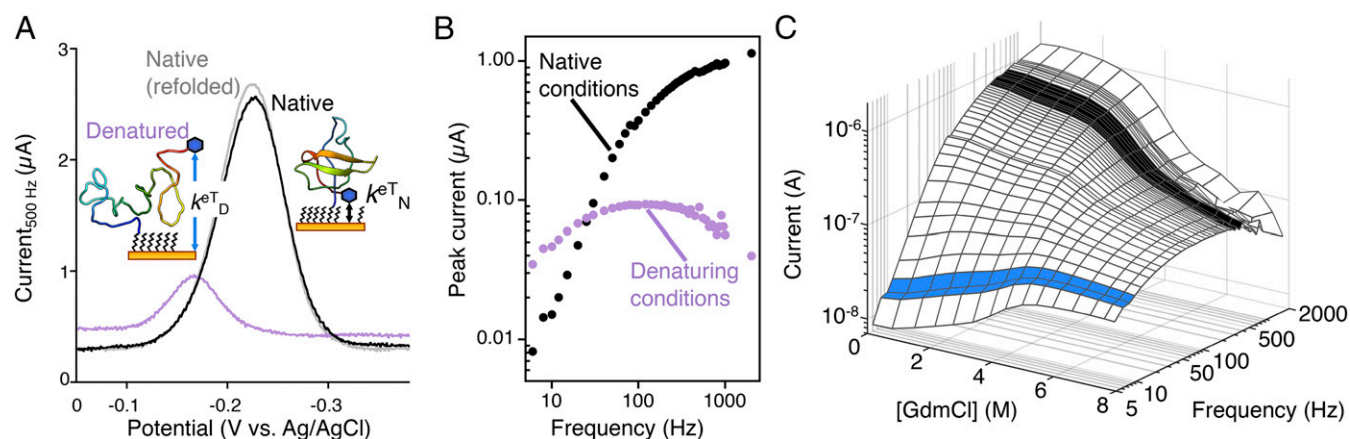
Fig. 2. Measuring folding thermodynamics of surface-tethered proteins by square-wave voltammetry. (*A*) To follow the chemical unfolding of the surface-attached protein, we use square-wave voltammetry to monitor electron transfer between its redox reporter and the surface. Because the reporter is positioned so that its rate of electron transfer differs between the folded (k^{eT}_N, black arrow) and unfolded (k^{eT}_D, blue arrow) states, the observed current changes upon denaturation (the data shown were obtained at a square-wave frequency of 500 Hz). Critically, the denaturant-induced unfolding of the surface-attached protein is reversible (compare gray and black voltammograms; see also *SI Appendix*, Fig. S3). (*B*) Because the current observed at a given square-wave frequency is dependent on the rate of the electron transfer, the difference in current between native and denaturing (7.8 M GdmCl) conditions is a strong function of square-wave frequency (see also *SI Appendix, Signal Optimization* and Figs. S2 and S5). (*C*) Specifically, the measured current is dominated by the slower electron transfer of the unfolded state at low square-wave frequencies (blue highlight), as seen from the increase in peak current with increasing denaturant concentration, a trend that is reversed at higher square-wave frequencies that sample faster electron transfer from the folded state (black highlight). Intermediate frequencies sample electron transfer from both states and consequently do not produce well-resolved denaturation curves. As a control, the electrochemistry of a methylene blue attached directly to the SAM (instead of via a protein) is effectively independent of denaturant concentration (*SI Appendix*, Fig. S5).

is, the redox potential of methylene blue is below the best estimate of the potential of zero charge for a hydroxyl-terminated six-carbon monolayer on gold (27), and thus, while our hydroxyl-terminated surface is, formally, neutral, the potential we apply to "interrogate" the methylene blue renders the surface slightly negatively charged. As the protein, too, is net negatively charged (adopting a net charge of −8 at the pH we employ), repulsion between the protein and the negatively charged surface should reduce the stability of its native state by favoring the formation of the more expanded, unfolded state. Similar electrostatic destabilization is observed when DNA, which is, of course, much more highly negatively charged, is attached to the same hydroxyl-terminated surface (26). A test of this hypothesis would be to measure the protein's folding free energy at low salt, under the argument that such repulsion would become more significant as the ionic strength decreases. To test this, we have also monitored the urea-induced unfolding of the protein, and find that, as expected, surface attachment is more destabilizing at lower ionic strength (*SI Appendix*, Fig. S4 *A* and *B*). This said, however, the urea *m*-value of FynSH3 is quite small, rendering it possible to determine the folding free energy of the surface-bound protein with confidence only over a narrow of ionic strengths (*SI Appendix*, Fig. S4C). It thus remains unclear the extent to which electrostatics contributes to the unfavorable interactions that are counteracting the (presumably) favorable excluded volume effects associated with surface attachment.

Discussion

Here we have measured the thermodynamic consequences of protein−surface interactions using the FynSH3 domain on a hydroxyl-terminated alkane-thiol-on-gold monolayer as our model system. For this protein−surface pair, we find that surface attachment is destabilizing by on the order of 2 kJ/mol when we use GdmCl as the denaturant, an observation we attribute to cancelation of a larger—and stabilizing—excluded volume effect by destabilizing interactions with the surface. Prior work with surface-bound nucleic acids (26) suggests that this could arise at least in part due to electrostatic interactions between the surface and positively and negatively

charged amino acids in the protein. With regard to this, it is important to remember that, at ionic strengths above a few tens of millimolars, the formation of an electric double layer causes the vast majority of the potential drop over charged surfaces to occur over only a few nanometers. Given that moving a single charge through a 10-mV potential produces a 1-kJ/mol change in free energy, the magnitude of such electrostatic effects can easily match typical protein stabilities, suggesting that electrostatic effects could be a significant contributor to the oft-seen unfolding of proteins when they are attached to artificial surfaces. This said, the discrepancy could also arise due to specific chemical interactions with the surface (e.g., hydrophobic, hydrogen bonding) that are better accommodated by the unfolded state (13), as the flexibility of this state allows it to conform more closely to the surface.

While the thermodynamic consequences of protein−surface interactions have long been the subject of theoretical exploration (23–25, 28, 29), they have seen relatively little quantitative experimental exploration. Specifically, among the few previous experimental measurements of surface−protein interactions, we find only two that describe the folding free energies of well-defined, single-chain biomolecules site-specifically attached to macroscopic surfaces. In these, Zare and coworkers (30) and Yi and coworkers (31) employed surface plasmon resonance to, respectively, monitor the urea-induced unfolding of cytochrome *c* linked to bare gold via a cysteine thiol and superoxide dismutase linked to a carboxyl-terminated SAM on gold via a random subset of its 11 lysines. Both groups reported that their surface-attached protein is destabilized relative to in solution. Regrettably, however, the conditions the two groups employed in their surface experiments differed from those used in bulk solution, rendering comparison between solution and surface folding thermodynamics—as well as comparison with our results—difficult. In related work, Möller, Nienhaus, and coworkers (32, 33) used Förster resonance energy transfer to monitor the urea-induced denaturation and subsequent refolding of surface-attached RNase H. They reported near-perfect refolding yields on (presumably uncharged) polyethylene surfaces, but failed to measure folding free energies. Guo and coworkers (34) likewise used immunochemistry to monitor the refolding of surface-attached
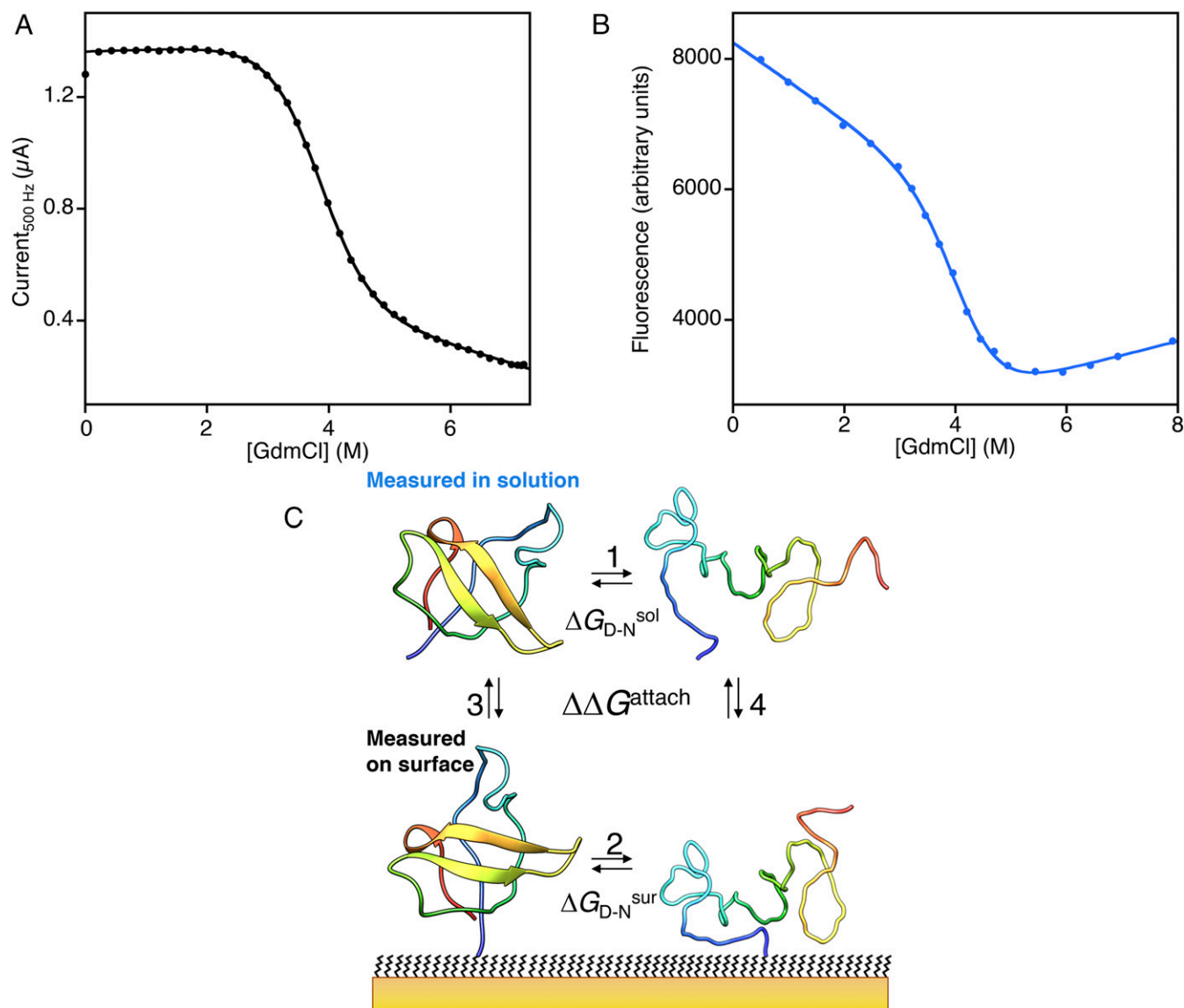
Fig. 3. Comparison of equilibrium unfolding curves of FynSH3 obtained under equivalent conditions when (*A*) site-specifically attached to our surface or (*B*) in bulk solution (monitored via tryptophan fluorescence). The *m*-value is effectively indistinguishable between the two, suggesting that the change in solvent-accessible surface area associated with unfolding is not affected by surface attachment (37). (*C*) Comparison of the folding free energy of the surface-attached protein (ΔG_{D-N}^{sur}; equilibrium 2) and that of the protein free in bulk solution (ΔG_{D-N}^{sol}; equilibrium 1) informs on the thermodynamic consequences of any protein–surface interactions. Under the conditions employed (i.e., with GdmCl as denaturant), attachment to the surface has no net effect on the stability of this protein.

green fluorescent protein. While they, too, identified surfaces supporting reversible refolding (e.g., amine-terminated monolayers), once again, no effort was made at thermodynamic characterization.

Given the limited scope of prior studies and the paucity of quantitative experimental tools with which to study protein–surface interactions, we believe the approach described here will improve our ability to characterize the molecular-scale origins of interactions between proteins and specific macroscopic surfaces, including both technologically important surfaces (as used here) and surfaces that mimic biomembranes (16). Looking forward, our goal is to use the approach to construct experimentally vetted, molecularly and thermodynamically detailed models of protein–surface interactions that can be used to rationally optimize the biocompatibility of artificial surfaces used in biophysics, biomaterials, biosensors, and other biomolecule-based technologies.

Materials and Methods

The variant FynSH3 we employed was produced by introducing mutations encoding K105R, K108R, and S143C in the gene for residues 83 to 143 of human tyrosine protein kinase Fyn (UniProt ID P06241). An amino-terminal 6xHis-tag and a tobacco etch virus (TEV) protease site (MHHHHHHENLYFQG) were added for purification purposes, where the Gly residue in the TEV site is G83 of FynSH3, yielding a protein with the wild-type amino terminus after proteolysis. Gene synthesis, codon optimization, subcloning into a pET-3a vector using 5′ Nde1 and 3′ BamH1 restriction sites, and construct sequencing were performed by GenScript, Inc.

All proteins were overexpressed in *Escherichia coli* BL21(DE3) cells (New England Biolabs) after transformation by standard heat shock. Overexpression was for 5 h in lysogeny broth with 100 μg/mL of carbenicillin at 37 °C, 230 rpm on a G10 gyrorotary shaker (New Brunswick Scientific), and induced with 1 mM isopropyl β-D-1-thiogalactopyranoside at $OD_{600} > 0.5$. Cells were harvested at 5000 rpm in a JA-10 rotor (Beckman) in a J2-HS centrifuge (Beckman) and resuspended in 20 mM sodium phosphate, 25 mM imidazole, 500 mM
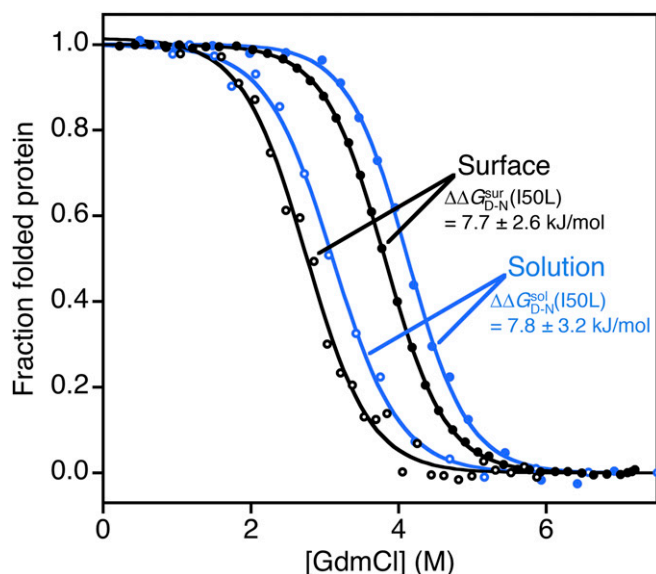
Fig. 4. The extent to which the I50L substitution alters the folding free energy of FynSH3 (I50L variant, open circles; FynSH3, closed circles) is the same for both the surface-attached protein (black) and the protein when it is free in bulk solution (blue). These results provide further support that our electrochemical approach is accurately measuring the thermodynamic stability of the surface-attached protein.

NaCl, pH 7.4. Cells expressing the I50L variant were resuspended and purified in presence of 6 M GdmCl.

Protein purification was at 4 °C unless otherwise stated. Cells were lysed by ultrasonication in presence of DNase (Sigma-Aldrich) and RNase (Roche). Cell debris was removed by 1 h of centrifugation at 11,000 rpm in a JA-20 rotor (Beckman) in a J2-HS centrifuge (Beckman), and the cleared, 0.2-μm-filtered supernatant loaded on a HisTrap HP column (GE Life Sciences). Elution was via a linear imidazole gradient up to 250 mM. FynSH3 containing fractions were identified on 16% Tris-Gly Novex SDS/PAGE gels (Thermo Fisher Scientific) by SafeStain staining (Thermo Fisher Scientific) and further purified on a Sephacryl S-100 size-exclusion column (GE Life Sciences) in 20 mM sodium phosphate, 130 mM NaCl, 1 mM (2-carboxyethyl)phosphine hydrochloride (TCEP), pH 7.0. Pure fractions were identified by SDS/PAGE as above and dialyzed into 20 mM sodium phosphate, 130 mM NaCl, pH 7.0. Protein concentration was determined by UV/visible spectroscopy. Protein and protein–methylene blue/anchor conjugate masses were verified by electrospray ionization mass spectrometry at the University of California, San Diego Molecular Mass Spectrometry Facility.

The his-tag was removed by overnight incubation at room temperature with one OD$_{280}$ unit of protease per six OD$_{280}$ units of FynSH3 in 50 mM sodium phosphate, 0.5 mM EDTA, 1 mM dithiotreitol, pH 7.0. His-tag-free FynSH3 was separated from protease and uncleaved protein on a HisTrap column (GE Life Sciences), and dialyzed into 1× PBS, pH 7.4 (Sigma-Aldrich). His-tagged TEV protease was overexpressed and purified in-house by standard procedures (35).

Methylene blue conjugation to C143 was performed under gentle mixing overnight at room temperature in the dark in PBS, pH 7.4 (Sigma-Aldrich), using a 2.5× molar excess of ATTO-MB2 maleimide derivative of methylene blue (ATTO-TEC GmbH) to 50 μM to 100 μM purified FynSH3 lacking His-tag; 1 mM TCEP was added before labeling. Excess methylene blue was removed by dialysis against 20 mM sodium phosphate, 130 mM NaCl, pH 7.0. Unlabeled protein was removed using a Phenyl Sepharose SP hydrophobic interaction chromatography column (GE Life Sciences) with a linear gradient of 1 M to 0 M ammonium sulfate in 50 mM sodium phosphate, pH 7.0. Protein conjugate fractions were identified using SDS/PAGE and a combination of in-gel methylene blue fluorescence detection using the Cy5 channel of a Typhoon laser scanner (GE Life Sciences) followed by Coomassie staining. Pure protein–methylene blue conjugate fractions display a single band visible by both methylene blue fluorescence and Coomassie staining, with a migration distance corresponding to the molecular mass of the conjugate. Fractions containing unreacted dye are not stained by Coomassie and only show a single methylene blue fluorescence band at ∼500 Da, while unconjugated protein yields no fluorescence signal.

The mercaptoheptanoic acid anchor was synthesized using established procedures (*SI Appendix*, Fig. S1). Its aliphatic segment matches six methylene units of our 6-mercapto-1-hexanol SAM (*SI Appendix*, Fig. S1), which prevents burial of the amide bond to the protein (16). Conjugation to methylene-blue-modified SH3 was done with a 40× molar excess of anchor in 20 mM sodium phosphate, 130 mM NaCl, pH 7.0 at 4 °C overnight under gentle mixing. Unreacted anchor was removed by dialysis against 20 mM sodium phosphate, 130 mM NaCl, 0.5 mM TCEP, pH 7.0 in a 3,000-Da cutoff slide-a-lyzer membrane (Thermo Fisher Scientific).

Direct conjugation of an alkyl thiol anchor to the ATTO-MB2 maleimide derivative of methylene blue (*SI Appendix*, Figs. S1 and S5) for control studies was as previously described (36). The conjugate was deposited using the same protocol as for the protein (below).

Polycrystalline gold disk electrodes (2 mm diameter; Buehler) were cleaned by polishing with a Microcloth (2 inches to 7/8 inches) in a 1-μm mono-crystalline diamond suspension, sonicated in ethanol, polished using a 0.05-μm aluminum slurry (Buehler), and sonicated in ethanol. Subsequently, electrochemical cleaning was performed by oxidation and reduction cycling in (*i*) 0.5 M NaOH (−0.4 to −1.35 V), (*ii*) 0.5 M H$_2$SO$_4$ (0 V to 2 V), (*iii*) 0.5 M H$_2$SO$_4$ (0 V to −0.35 V), and (*iv*) 0.5 M H$_2$SO$_4$ (−0.35 V to +1.5 V).

The protein was incubated in 20 mM sodium phosphate, 4 mM TCEP, 130 mM NaCl, pH 7.0 to reduce the surface-anchoring thiol, and attached to the cleaned gold electrode surface by incubating it in 1.4 μM protein for 10 min at room temperature in 20 mM sodium phosphate, 130 mM NaCl, 50 μM TCEP, pH 7.0. The protein-functionalized surface was washed with deionized water and incubated overnight in 5 mM 6-mercapto-1-hexanol (Sigma-Aldrich) in 20 mM sodium phosphate, 130 mM NaCl, pH 7.0 to form the SAM. Subsequent steps were performed with this buffer composition unless otherwise noted. The SAM-coated electrodes were incubated for 4 h in buffer with 7 M GdmCl, 1 mM 6-mercapto-1-hexanol to remove non-specifically adsorbed protein and SAM-coat any patches of bare gold exposed due to protein desorption. Before use, each electrode was washed for 20 min in buffer with 1 M NaCl, 1 mM 6-mercapto-1-hexanol followed by 7 M GdmCl in buffer with 1 mM 6-mercapto-1-hexanol. These two steps were repeated three more times. Each electrode was interrogated 50 times by square-wave voltammetry in fresh buffer containing 50 μM 6-mercapto-1-hexanol at 60 Hz, 25 mV amplitude using the same potential window as in the denaturation experiments before initiating chemical melt experiments.

We determined the electroactive area of each electrode by cycling the potential twice between −0.35 V and 1.5 V in 0.05 M H$_2$SO$_4$ at 0.1 V·s$^{−1}$ scan rate and integrating the area of the gold oxide reduction peak in the final segment. From this area determination and the methylene blue peak area obtained by cyclic voltammetry at 0.1 V·s$^{−1}$ scan rate, we estimated an average packing density on the surface of 1.0 ± 0.2 × 10^{11} molecules per square centimeter. This corresponds to spacing in the dilute regime, whether based on the 32 × 24 Å cross-section of the folded protein or the 240-Å contour length of the unfolded protein. That is, adjacent proteins are far enough apart to minimize protein–protein interactions.

Equilibrium denaturation curves were obtained using ultrapure urea (MP Biomedicals) or GdmCl (Thermo Fisher Scientific). We performed these on the surface using two Hamilton 500C dual-syringe dispensers synchronized with a CH Instruments 660D potentiostat and a BASi C3 Cell Stand (Bioanalytical Systems, Inc.). This setup allows for automated consecutive unfolding and refolding titrations. Experiments were started in buffer, subsequently titrating in denaturant; 50 μM 6-mercapto-1-hexanol was included in the buffer to minimize baseline drift. The system was equilibrated under thorough but gentle mixing for 10 min before measurement at each denaturation concentration, and stirring was paused during measurements to reduce electrical noise. Square-wave voltammograms were recorded between −0.05 V and −0.38 V at 25-mV amplitude in 5 mL total bulk solution volume with a platinum counter electrode and an Ag/AgCl reference electrode with saturated potassium chloride. To determine the folding free energy, we monitored the peak current at the redox potential of methylene blue as a function of GdmCl or urea concentration. Peak currents were evaluated using MatLab (The MathWorks, Inc.) and CHI Version 14.06 (CH Instruments). The denaturation curves were fitted to a standard two-state folding model (18) in Kaleidagraph (Synergy Software),

$$I_{obs} = \frac{a[\text{denaturant}] + I_N + (b[\text{denaturant}] + I_D)10^{m_{D-N}([\text{denaturant}]-MP^{eq})}}{1 + 10^{m_{D-N}([\text{denaturant}]-MP^{eq})}} \quad [1]$$

where I_{obs} is the observed signal, I_N and I_D are the signal intensities of folded and unfolded protein, respectively, a and b are the baseline slopes, and MP^{eq} is the denaturation midpoint. The free energy of folding is defined as

Kurnik et al.

$$\Delta G_{D-N} = -RT \ln K_{D-N} = -RT \ln(m_{D-N} MP^{eq}) \qquad [2]$$

where $K_{D-N} = [D]/[N]$ is the equilibrium constant for the folding reaction. D and N represent the monomers in the denatured and native states, respectively.

Solution-phase measurements were made under conditions equivalent to those employed for the surface experiments using a Cary Eclipse Fluorimeter with 280-nm excitation and 300- to 440-nm emission, and data were fitted to Eq. **1**. Of note is that modifying FynSH3 with methylene blue and the thiol surface anchor does not alter its *m*-value or folding free energy (*SI Appendix*, Fig. S6). We therefore performed our follow-up solution-phase experiments with protein lacking reporter and anchor. Each denaturant concentration was prepared as a discrete sample by mixing of different volume ratios of denaturant and buffer stock solutions containing 1 μM protein.

1. Papanastasiou M, et al. (2013) The *Escherichia coli* peripheral inner membrane proteome. *Mol Cell Proteomics* 12:599–610.
2. Ott M, Gogvadze V, Orrenius S, Zhivotovsky B (2007) Mitochondria, oxidative stress and cell death. *Apoptosis* 12:913–922.
3. Oldham WM, Hamm HE (2008) Heterotrimeric G protein activation by G-protein-coupled receptors. *Nat Rev Mol Cell Biol* 9:60–71.
4. Serra-Batiste M, et al. (2016) Aβ42 assembles into specific β-barrel pore-forming oligomers in membrane-mimicking environments. *Proc Natl Acad Sci USA* 113:10866–10871.
5. Winner B, et al. (2011) In vivo demonstration that alpha-synuclein oligomers are toxic. *Proc Natl Acad Sci USA* 108:4194–4199.
6. Andreasen M, Lorenzen N, Otzen D (2015) Interactions between misfolded protein oligomers and membranes: A central topic in neurodegenerative diseases? *Biochim Biophys Acta* 1848:1897–1907.
7. Hlady V, Buijs J (1996) Protein adsorption on solid surfaces. *Curr Opin Biotechnol* 7:72–77.
8. Gray JJ (2004) The interaction of proteins with solid surfaces. *Curr Opin Struct Biol* 14:110–115.
9. Katoch J, et al. (2012) Structure of a peptide adsorbed on graphene and graphite. *Nano Lett* 12:2342–2346.
10. Gruian C, Vanea E, Simon S, Simon V (2012) FTIR and XPS studies of protein adsorption onto functionalized bioactive glass. *Biochim Biophys Acta* 1824:873–881.
11. Raut VP, Agashe MA, Stuart SJ, Latour RA (2005) Molecular dynamics simulations of peptide-surface interactions. *Langmuir* 21:1629–1639.
12. Zhuang Z, Jewett AI, Soto P, Shea JE (2009) The effect of surface tethering on the folding of the src-SH3 protein domain. *Phys Biol* 6:015004.
13. Levine ZA, Fischer SA, Shea JE, Pfaendtner J (2015) Trp-cage folding on organic surfaces. *J Phys Chem B* 119:10417–10425.
14. Plaxco KW, et al. (1998) The folding kinetics and thermodynamics of the Fyn-SH3 domain. *Biochemistry* 37:2529–2537.
15. Maxwell KL, Davidson AR (1998) Mutagenesis of a buried polar interaction in an SH3 domain: Sequence conservation provides the best prediction of stability effects. *Biochemistry* 37:16172–16182.
16. Love JC, Estroff LA, Kriebel JK, Nuzzo RG, Whitesides GM (2005) Self-assembled monolayers of thiolates on metals as a form of nanotechnology. *Chem Rev* 105:1103–1169.
17. Lubin AA, Plaxco KW (2010) Folding-based electrochemical biosensors: The case for responsive nucleic acid architectures. *Acc Chem Res* 43:496–505.
18. Tanford C (1968) Protein denaturation. *Adv Protein Chem* 23:121–282.
19. Fersht AR (1999) *Structure and Mechanism in Protein Science: A Guide to Enzyme Catalysis and Protein Folding* (WH Freeman, New York).
20. Arold S, et al. (1997) The crystal structure of HIV-1 Nef protein bound to the Fyn kinase SH3 domain suggests a role for this complex in altered T cell receptor signaling. *Structure* 5:1361–1372.
21. Northey JG, Di Nardo AA, Davidson AR (2002) Hydrophobic core packing in the SH3 domain folding transition state. *Nat Struct Biol* 9:126–130.
22. Fitzkee NC, Rose GD (2004) Reassessing random-coil statistics in unfolded proteins. *Proc Natl Acad Sci USA* 101:12497–12502.
23. Dolan AK, Edwards SF (1974) Theory of the stabilization of colloids by adsorbed polymer. *Proc R Soc A* 337:509–516.
24. Zhou HX, Dill KA (2001) Stabilization of proteins in confined spaces. *Biochemistry* 40:11289–11293.
25. Chen YC, Luo MB (2007) Monte Carlo study on the entropy of tail-like polymer chain with one end attached to flat surface. *Int J Mod Phys B* 21:1787–1795.
26. Watkins HM, Vallée-Bélisle A, Ricci F, Makarov DE, Plaxco KW (2012) Entropic and electrostatic effects on the folding free energy of a surface-attached biomolecule: An experimental and theoretical study. *J Am Chem Soc* 134:2120–2126.
27. Rentsch S, Siegenthaler H, Papastavrou G (2007) Diffuse layer properties of thiol-modified gold electrodes probed by direct force measurements. *Langmuir* 23:9083–9091.
28. Dobrynin AV, Obukhov SP, Rubinstein M (1999) Long-range multichain adsorption of polyampholytes on a charged surface. *Macromolecules* 32:5689–5700.
29. Dobrynin AV, Colby RH, Rubinstein M (2004) Polyampholytes. *J Polym Sci B* 42:3513–3538.
30. Chah S, Kumar CV, Hammond MR, Zare RN (2004) Denaturation and renaturation of self-assembled yeast iso-1-cytochrome c on Au. *Anal Chem* 76:2112–2117.
31. Kang T, Hong S, Choi I, Sung JJ, Yi J (2008) Urea-driven conformational changes in surface-bound superoxide dismutase. *Bull Korean Chem Soc* 29:1451–1458.
32. Groll J, et al. (2004) Biofunctionalized, ultrathin coatings of cross-linked star-shaped poly(ethylene oxide) allow reversible folding of immobilized proteins. *J Am Chem Soc* 126:4234–4239.
33. Heyes CD, Groll J, Möller M, Nienhaus GU (2007) Synthesis, patterning and applications of star-shaped poly(ethylene glycol) biofunctionalized surfaces. *Mol Biosyst* 3:419–430.
34. Holtz B, Wang Y, Zhu XY, Guo A (2007) Denaturing and refolding of protein molecules on surfaces. *Proteomics* 7:1771–1774.
35. Becker AH, Oh E, Weissman JS, Kramer G, Bukau B (2013) Selective ribosome profiling as a tool for studying the interaction of chaperones and targeting factors with nascent polypeptide chains and ribosomes. *Nat Protoc* 8:2212–2239.
36. Dauphin-Ducharme P, et al. (2017) Simulation-based approach to determining electron transfer rates using square-wave voltammetry. *Langmuir* 33:4407–4413.
37. Myers JK, Pace CN, Scholtz JM (1995) Denaturant m values and heat capacity changes: Relation to changes in accessible surface areas of protein unfolding. *Protein Sci* 4:2138–2148.

BIOPHYSICS AND COMPUTATIONAL BIOLOGY